Bevington, P. R. (1969) *Data Reduction and Error Analysis for the Physical Sciences*, McGraw-Hill, New York.
Brandts, J. F., Oliveira, R. J., & Westort, C. (1970) *Biochemistry 9*, 1038.
Bruckman, T. G. (1977) Ph.D. Thesis, Cornell University, Ithaca, NY.
Clegg, R. M., & Maxfield, B. W. (1976) *Rev. Sci. Instrum. 47*, 1383.
Clegg, R. M., Elson, E. L., & Maxfield, B. W. (1975) *Biopolymers 14*, 883.
Champion, P. M., & Albrecht, A. C. (1979) *J. Chem. Phys. 71*, 1110.
Dill, K. A. (1985) *Biochemistry 24*, 1501.
Drew, H. E., & Dickerson, R. E. (1978) *J. Biol. Chem. 253*, 8420.
Dyson, H. J., & Beattie, J. K. (1982) *J. Biol. Chem. 257*, 2267.
Edsall, J. T., & McKenzie, H. A. (1983) *Adv. Biophys. 16*, 53.
Eigen, M., & de Maeyer, L. (1963) *Technique of Organic Chemistry* (Friess, S. L., Lewis, E. S., & Weissberger, A., Eds.) Vol. VIII, Part 2, p 895, Wiley-Interscience, New York.
Folin, M., Azzi, A., & Tamburro, A. M. (1972) *Biochem. Biophys. Acta 285*, 337.
Halvorson, H. R. (1979) *Biochemistry 18*, 2480.
Harbury, H. A., & Loach, P. A. (1959) *Proc. Natl. Acad. Sci. U.S.A. 45*, 1344.
Ikai, A., Fish, W. W., & Tanford, C. (1973) *J. Mol. Biol. 73*, 165.
Jeng, M.-F., & Englander, S. W. (1991) *J. Mol. Biol. 221*, 1045.
Kauzmann, W. (1959) *Adv. Protein Chem. 14*, 1.
Kauzmann, W. (1987) *Nature (London) 325*, 763.
Lee, S., Karplus, M., Bashford, D., & Weaver, D. (1987) *Biopolymers 26*, 481.
Macgregor, R. B., & Clegg, R. M. (1987) *Biopolymers 26*, 2103.
Macgregor, R. B., Clegg, R. M., & Jovin, T. M. (1985) *Biochemistry 24*, 5503.
Myer, Y. P. (1980) *Biochemistry 19*, 199.
Nall, B. T. (1983) *Biochemistry 22*, 1423.
Nall, B. T., & Landers, T. A. (1981) *Biochemistry 20*, 5403.
Nanzyo, N., & Sano, S. (1968) *J. Biol. Chem. 243*, 3431.
Privalov, P. L. (1979) *Adv. Protein Chem. 33*, 167.
Privalov, P. L., & Gill, S. J. (1988) *Adv. Protein Chem. 39*, 191.
Pryse, K. M. (1988) Ph.D. Thesis, Cornell University, Ithaca, NY.
Roder, H., Elöve, G. A., & Englander, S. W. (1991) *Nature (London) 335*, 700.
Schellman, J. A. (1978) *Biopolymers 17*, 1305.
Sreenathan, B. R., & Taylor, C. P. S. (1971) *Biochem. Biophys. Res. Commun. 42*, 1122.
Stellwagen, E. (1968) *Biochemistry 7*, 2496.
Tsong, T. Y. (1974) *J. Biol. Chem. 249*, 1988.
Tsong, T. Y. (1975) *Biochemistry 14*, 1542.
Tsong, T. Y. (1976) *Biochemistry 15*, 5467.
Tsong, T. Y. (1977) *J. Biol. Chem. 252*, 8778.
Williams, R. J. P. (1971) *Cold Spring Harbor Symp. Quant. Biol. 36*, 53.

Determination of the Molecular Dynamics of Alamethicin Using ^{13}C NMR: Implications for the Mechanism of Gating of a Voltage-Dependent Channel†

Laurie P. Kelsh, Jeffrey F. Ellena, and David S. Cafiso*
Department of Chemistry and Biophysics Program, University of Virginia, Charlottesville, Virginia 22901
Received August 2, 1991; Revised Manuscript Received December 30, 1991

ABSTRACT: Alamethicin is a channel-forming peptide antibiotic that produces a highly voltage-dependent conductance in planar bilayers. To provide insight into the mechanisms for its voltage dependence, the dynamics of the peptide were examined in solution using nuclear magnetic resonance. Natural-abundance ^{13}C spin–lattice relaxation rates and ^{13}C–^{1}H nuclear Overhauser effects of alamethicin were measured at two magnetic field strengths in methanol. This information was interpreted using a model-free approach to obtain values for the overall correlation times as well as the rates and amplitudes of the internal motions of the peptide. The picosecond, internal motions of alamethicin are highly restricted along the peptide backbone and indicate that it behaves as a rigid helical rod in solution. The side chain carbons exhibit increased segmental motion as their distance from the peptide backbone is increased; however, these motions are not unrestricted. Methyl group dynamics are also consistent with the restricted motions observed for the backbone carbons. There is no evidence from these dynamics measurements for a hinged motion of the peptide about proline-14. Alamethicin appears to be slightly less structured in methanol than in the membrane; as a result, alamethicin is also expected to behave as a rigid helix in the membrane. This suggests that the gating of this peptide involves changes in the orientation of the entire helix, rather than the movement of a segment of the peptide backbone.

Voltage-dependent conformational transitions in membrane proteins are of central importance to many processes such as information transfer in the nervous system and energy transduction. As a result, the elucidation of these mechanisms even in simple model systems has been actively pursued. Alamethicin is a small, 20 amino acid peptide that produces a dramatic voltage-dependent conductance when incorporated into planar bilayers or lipid vesicles. This voltage dependence and alamethicin's tractable size have made it an attractive

† This work was supported by a grant from the National Institutes of Health (GM-35215 to D.S.C.).

0006-2960/92/0431-5136$03.00/0

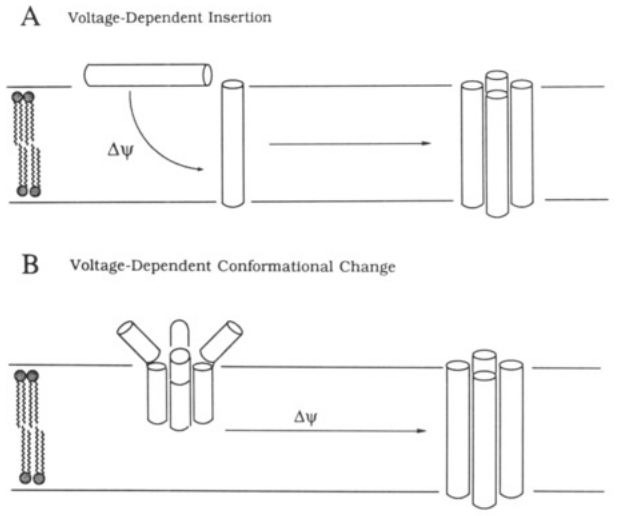

FIGURE 1: Two examples of models for the voltage-dependent gating of alamethicin that place different requirements on the dynamics of the peptide secondary structure. (A) A model that involves a change in the orientation of the peptide helix from a parallel to a perpendicular orientation in the presence of an applied transmembrane field. (B) A model that requires a change in the orientation of the N-terminal segment of alamethicin with an applied transmembrane field. In model A, the peptide can remain a relatively rigid rod. In model B, flexibility about the helix backbone is required.

model for examining membrane–protein electrostatic interactions and voltage-dependent conformational transitions. Alamethicin is rich in helix-favoring residues such as α-aminoisobutyric acid (Aib),[1] and recent structural studies of alamethicin have used CD (Vogel, 1987; Jung et al., 1975; Cascio & Wallace, 1988), Raman (Vogel, 1987), FTIR (Fringeli & Fringeli, 1979), and NMR (Banerjee & Chan, 1983; Banerjee et al., 1983; Esposito et al., 1987) spectroscopies to elucidate its solution and membrane conformations. Nearly all these reports are consistent with an N-terminal α-helical region that extends through residue 10 or 11. This structural paradigm is found to occur both in methanol and in lipid bilayers. The structure of the C-terminal region is less well characterized. X-ray and NMR data indicate that the C-terminal region is an extended helix (Fox & Richards, 1982; Esposito et al., 1987), while Raman and CD data provide evidence for some β-sheet in this domain (Hall et al., 1984). In addition, the structure in the membrane-bound state has been reported to be slightly more ordered than the solution structure (Vogel, 1987).

The molecular mechanism by which alamethicin induces a voltage-dependent ion conductance in lipid bilayers is currently not understood. Because of the strong concentration dependence of this conductance, it is generally believed that formation of the channel involves the association of approximately 6–12 monomers; however, a number of strikingly different models have been proposed to explain the gating of alamethicin. In one intriguing model, alamethicin conductance becomes voltage-dependent because its partitioning to bilayers is voltage-dependent (Schwarz, et al., 1986). Recent work argues against this model. Evidence for a voltage-dependent partitioning has not been found (Wille et al., 1989), and alamethicin can promote a highly nonlinear voltage-dependent conductance in vesicle systems under conditions where all the peptide is membrane-bound (Archer & Cafiso, 1991). A related model (see Figure 1A) that appears to be more likely involves the voltage-dependent movement of alamethicin from an orientation parallel to the membrane surface to a transmembrane orientation (Bauman & Mueller, 1974; Boheim, 1974). In a model more recently proposed (Boheim et al., 1983; Menestrina et al., 1986), the voltage-dependent event involves a change in the organization of the alamethicin aggregate. In this model, the closed state of the channel is composed of an antiparallel aggregate of helical monomers. In response to an applied potential, one of the monomers undergoes a "flip-flop" which promotes a dipole repulsion in the aggregate and opens the channel. Another type of model that has been proposed incorporates a conformational change in the monomer structure. For example, Hall et al. (1984) proposed that alamethicin formed an aggregate resembling a β-barrel with both the C- and N-termini at the same interface. In response to an applied potential, the N-terminus crosses the bilayer, and the channel is opened. This folded backbone is brought about by a turn at Pro-14. Similarly, Fox and Richards (1982) proposed that the closed state is an aggregate of helices with the N-termini in the bilayer and the C-termini bent away from the channel axis into the solvent (see Figure 1B). The application of voltage causes the disordered C-termini to become helical, reorient by bending at Pro-14, and insert completely into the bilayer. While these last two models require some internal motion in the monomer, the other models described above do not require any internal dynamics in the monomer.

An examination of the local internal motions of the backbone and side chain atoms is important to an understanding of the relationship between protein structure and function (Brooks et al., 1988; Karplus & Dobson, 1986; Williams, 1989; Brunger et al., 1987). In fact, these motions may be viewed as a link between the static, rigid picture of proteins and peptides provided by X-ray and NMR structural studies and the mechanisms of protein function. NMR relaxation provides a unique means of analyzing the motions available to a molecule. An analysis of the relaxation data, i.e., T_1^{-1}, T_2^{-1}, and nuclear Overhauser effect (NOE) for individual nuclei can yield information about the overall and local motions present in a given system. This technique has been successfully used to evaluate motion in lipid micelles and bilayers [see, for example, Lindman et al. (1987) and Mayer et al. (1990) and references cited therein], peptides and proteins (Dellwo & Wand, 1989; Weaver et al., 1988, 1989; Henry et al., 1986; Kay et al., 1989; Clore et al., 1990), and DNA (Lipari & Szabo, 1981a). Earlier studies relied on some knowledge of the type of motion(s) present in order to devise functional forms for the interpretation of relaxation data (Woessner, 1962; London & Avitable, 1978; Wittebort & Szabo, 1978; Lipari & Szabo, 1981b). More recently, these studies have utilized the "model-free" approach devised by Lipari and Szabo (1982a,b). This method fits the numerical data without any assumptions as to the type of motion(s) involved, and the interpretation of the data is accomplished by a comparison of the calculated parameters with those predicted by specific models for molecular motion. The validity of the calculated parameters can be evaluated, which allows a qualitative assessment of the fit. This approach provides a powerful method to evaluate molecular motions on the NMR time scale.

A determination of the internal motions of the alamethicin backbone should provide insight into the mechanism by which this peptide channel is gated. For two of the models described

[1] Abbreviations: Aib, α-aminoisobutyric acid; CD, circular dichroism; FTIR, Fourier transform infrared; NMR, nuclear magnetic resonance; T_1, spin–lattice relaxation time; NOE, nuclear Overhauser effect; HOHAHA, homonuclear Hartmann–Hahn; HMBC, heteronuclear multiple bond correlation; CSA, chemical shielding anisotropy; TFA, trifluoroacetic acid.

above, the voltage-dependent conformational transition requires flexibility along the backbone of alamethicin (for example, near Pro-14 in the β-barrel model), whereas other models for alamethicin gating do not necessitate conformational flexibility in the backbone. In this report, the motions of the channel-forming peptide alamethicin are examined by measuring and analyzing the ^{13}C NMR spin–lattice relaxation and NOE data obtained at two magnetic field strengths using the model-free approach. The data and analysis that is presented here provide evidence that the backbone of alamethicin is rigid and lacks conformational flexibility in methanol. Because of the similarities between the methanol and membrane structures, the state of the peptide in solution has implications for the behavior of alamethicin in membranes.

Experimental Procedures

Materials. Alamethicin was purchased from Sigma (St. Louis, MO) and was purified by HPLC using a Vyadac (The Separations Group, Hesperia, CA) C18 semiprep reverse-phase column. The alamethicin fractions were eluted by using an isocratic solvent system consisting of 40% H_2O/60% acetonitrile containing 0.1% TFA. The elution profile showed two major components, one eluting at 17 min, the other at 25 min; these components were identified as Ac-NαPαAαAQαVαGLαPVααQQF-ol and Ac-NαPαAαQαVαGLαPVααQQF-ol by mass spectrometry. The fraction with Ala-6 was used throughout this study. T_1 and NOE measurements were made on an alamethicin sample at 15 mM in $^{12}CD_3OD$ (MSD Isotopes, St. Louis, MO); the pH of this sample was ~6.0 (uncorrected for ^2H isotope effect). Previous work that has been carried out on alamethicin in methanol indicates that it remains monomeric in this solvent, even at high concentrations (Esposito et al., 1987; Cascio & Wallace, 1988; Archer et al., 1991). This assumption is supported by the results obtained here, which indicate that the rotational rate for alamethicin in solution is consistent with the expected rotational rate of a monomer (see Discussion).

NMR Spectroscopy. ^1H and ^{13}C resonance assignments for alamethicin were made by using two-dimensional NMR methods at 500.13 MHz for ^1H and at 125.76 MHz for ^{13}C on a General Electric Omega 500. The ^1H assignments were made by using the double-quantum-filtered COSY (Piantini et al., 1982) and two-dimensional HOHAHA (Braunschweiler & Ernst, 1983; Bax & Davis, 1985) experiments. Z-filtering (Rance, 1987) and a 60-ms MLEV-17 mixing pulse were used in the HOHAHA experiment. For this experiment, two 64 × 512 × 1024 data sets were collected in the hypercomplex mode (Haberkorn et al., 1982). Single-bond heteronuclear correlations were obtained by using the HMQC sequence of Bax and Summers (1986) were GARP ^{13}C decoupling (Shaka et al., 1985). The ^{13}C frequency was sampled from 15 to 85 ppm, and two 128 × 256 × 2048 data sets were collected in the hypercomplex mode (Haberkorn et al., 1982). The first t_1 interval was adjusted such that data sampling began at a time equal to half the t_1 dwell time to provide a flat base plane after processing (Bax et al., 1991). The HMBC sequence (Bax & Summers, 1986) was used to obtain multiple bond coupling information, and a 128 × 256 × 2048 data set was collected and processed in the magnitude mode. This experiment was particularly useful in resolving correlations involving the Pro-2 and -14 β-carbons and the Gln-7, -18, and -19 β- and γ-carbons. All data were processed with the FTNMR data analysis package (Hare Research, Inc., Woodinville, WA).

One-dimensional ^{13}C T_1 and NOE measurements were made at 125.76 MHz on the Omega 500 and at 75.5 MHz on a General Electric GN300 spectrometer. T_1 data were collected by using the inversion recovery sequence, 180–τ–90–ACQ. A typical T_1 measurement consisted of 15 data sets collected for τ values of 20, 40, 80, 160, 320, 540, and 720 ms and 1.0, 1.5, 2.0, 3.0, 4.0, 6.0, 8.0, and 10.0 s. For each data set, 1024 scans of 16K or 32K points covering frequencies between 15 and 85 ppm were collected with modulated ^1H decoupling and with the total delay between scans greater than $10T_1$. Data sets were interleaved in order to average time-dependent signal changes over all τ values. The data were fit with a three-parameter exponential function using the NMR1 software (New Methods Research, Inc., Syracuse, NY). NOE measurements were made by dividing the signal intensity obtained in the presence of continuous ^1H decoupling to that obtained with ^1H decoupling only during the acquisition. A typical data set consisted of 2048 scans of 16K or 32K points covering 15–85 ppm collected with the total time between scans approximately equal to $10–20T_1$. Data collection was alternated between that with ^1H decoupling and that without to average time-dependent changes in the signal. Three T_1 and two to four NOE values were obtained at each frequency. Nearly all protonated carbon resonances were resolved at both frequencies. Those resonances which were degenerate, namely, the Pro-2/Val-9 α-carbons and the Leu-12/Ala-4 α-carbons, were not used in the subsequent analysis. In addition, the Gln-7 α-carbon was not used for analysis due to significant overlap with the (quaternary) Aib α-carbon resonances.

Analysis of NMR Relaxation Data. The analysis of ^{13}C nuclear relaxation is reasonably straightforward because of the relatively low abundance of the nucleus and because the spectra are recorded under simultaneous modulated ^1H decoupling. Under these conditions, ^{13}C nuclei relax predominantly through dipolar interactions with their bonded protons. In addition, the broad range of chemical shifts observed for ^{13}C and the observation of a single line for each resonance (under ^1H decoupling) provide well-resolved, easily interpreted spectra. In the analysis made here, contributions to the relaxation due to the chemical shielding anisotropy (CSA) will be ignored. For aliphatic carbons, $\Delta\sigma$ is expected to be approximately 20 ppm [see Dellwo and Wand (1989)]. At the frequencies used (125 MHz for ^{13}C), the CSA will make a contribution that is only a few percent of the total relaxation for carbons having the smallest relaxation rates found here.

The "model-free" method of Lipari and Szabo (1982a,b) was used to analyze the relaxation data. The formulation of the correlation function which describes molecular motion assumes only that the overall and internal motions are independent, and no assumptions are made as to the type, amplitude, or frequency of motion. The analysis of the NMR relaxation data was made here with two different models for the overall motion of the peptide: one that assumes an isotropic and another that assumes an anisotropic rotational diffusion. The correlation functions for the isotropic and anisotropic motion, $C_o^i(t)$ and $C_o^a(t)$, respectively, are described by

$$C_o^i(t) = (1/5)\exp(-t/\tau_M) \quad (1a)$$

$$C_o^a(t) = (1/5)[A\exp(-t/\tau_1) + (1 - A)\exp(-t/\tau_2)] \quad (1b)$$

where τ_M is the time constant for overall isotropic rotation, τ_1 and τ_2 are the time constants for anisotropic rotation, and A is a weighting factor for anisotropic rotation. For each type of overall motion, the internal motions are characterized by a time constant, τ_e, and a generalized order parameter, S, that mathematically define the internal correlation function, $C_I(t)$:

$$C_I(t) = S^2 + (1 - S^2)\exp(-t/\tau_e) \quad (2)$$

The corresponding spectral density functions are given by

$$J^{i}(\omega) = \frac{S^2\tau_M}{1 + (\omega\tau_M)^2} + \frac{(1 - S^2)\tau}{1 + (\omega\tau)^2} \text{ where } \frac{1}{\tau} = \frac{1}{\tau_M} + \frac{1}{\tau_e} \quad (3a)$$

$$J^{a}(\omega) = S^2\left[\frac{A\tau_1}{1 + (\omega\tau_1)^2} + \frac{(1 - A)\tau_2}{1 + (\omega\tau_2)^2}\right] + (1 - S^2) \times \left[\frac{A\tau_{1e}}{1 + (\omega\tau_{1e})^2} + \frac{(1 - A)\tau_{2e}}{1 + (\omega\tau_{2e})^2}\right] \text{ where } \frac{1}{\tau_{ie}} = \frac{1}{\tau_i} + \frac{1}{\tau_e} \text{ for } i = 1, 2 \quad (3b)$$

By using eq 3a,b along with equations that relate the observables T_1 and NOE to the spectral density function (see eq 4a,b), the correlation times and order parameters for overall

$$\frac{1}{T_1} = \frac{N}{20}\left(\frac{\gamma_H\gamma_C\hbar}{r^3}\right)^2 [J(\omega_H - \omega_C) + 3J(\omega_C) + 6J(\omega_H + \omega_C)] \quad (4a)$$

$$\text{NOE} = 1 + \frac{\gamma_H}{\gamma_C}\left[\frac{6J(\omega_H + \omega_C) - J(\omega_H - \omega_C)}{J(\omega_H - \omega_C) + 3J(\omega_C) + 6J(\omega_H + \omega_C)}\right] \quad (4b)$$

and internal motions can be specified. In eq 4a,b, N is the number of directly bonded hydrogens, γ_H and γ_C are the hydrogen and carbon magnetogyric ratios, respectively, $\hbar$ is Planck's constant, r is the C–H bond distance, and $J(\omega)$ are the spectral densities in terms of the angular resonant frequencies for ^{13}C (ω_C) and ^{1}H (ω_H).

Several assumptions regarding the rate and type of internal motions present in a system give rise to simplifications of eq 3a,b. When the fast motions are in the extreme narrowing limit, i.e., when $[(\omega_H + \omega_C)\tau_e]^2 \ll 1$ and $\tau_e \ll \tau_M(\tau_2)$, the second term in each equation reduces to $(1 - S^2)\tau_e$, which yields

$$J^{i}(\omega) = \frac{S^2\tau_M}{1 + (\omega\tau_M)^2} + (1 - S^2)\tau_e \quad (5a)$$

$$J^{a}(\omega) = S^2\left[\frac{A\tau_1}{1 + (\omega\tau_1)^2} + \frac{(1 - A)\tau_2}{1 + (\omega\tau_2)^2}\right] + (1 - S^2)\tau_e \quad (5b)$$

In addition, for the case where τ_e approaches 0, eq 5a,b can be further simplified to obtain

$$J^{i}(\omega) = \frac{S^2\tau_M}{1 + (\omega\tau_M)^2} \quad (6a)$$

$$J^{a}(\omega) = S^2\left[\frac{A\tau_1}{1 + (\omega\tau_1)^2} + \frac{(1 - A)\tau_2}{1 + (\omega\tau_2)^2}\right] \quad (6b)$$

For a given set of relaxation data, the appropriate spectral density form and parameters were determined by fitting the experimental data with a nonlinear optimization routine. In general, data fitting is an iterative process in which these observables, T_1 and NOE, are calculated for different sets of spectral density function parameters. An error function, given by eq 7, is then calculated, and it is this value that is minimized. For isotropic overall motion, the total error was calculated as the sum of the error function (eq 7) for seven α-carbons using the full spectral density function for isotropic motion (eq 3a) as τ_M was varied over 2 orders of magnitude. The minimum in the total error was determined, and the associated τ_M was then used for the calculation of $\{S^2, \tau_e\}$ pairs for every carbon. For anisotropic overall motion, the best A, τ_1, and τ_2 values were determined for the α-carbons by searching a $50 \times 100 \times 100$ grid using the anisotropic spectral density function in eq 5b. τ_1 and τ_2 were varied over 2 orders of magnitude, and A was varied from 0.02 to 1.0. The total error was evaluated as the sum of the error function for seven α-carbons at each point on the grid; the minimum error was evaluated, and the associated τ_1, τ_2, and A values were determined along with the $\{S^2, \tau_e\}$ pairs for each carbon position. With four independent measures of relaxation, T_1, and NOE at two frequencies, a unique solution to this set of nonlinear equations should be found if one exists (Lipari & Szabo, 1982a; Dellwo & Wand, 1989). The accuracy of the τ_M, τ_e, and S^2 values is related to the types of motions present. In general, if internal motions are in the fast regime, i.e., $(\omega\tau_e)^2 \ll 1$ and $\tau_e/\tau_M \leq 0.01$, then the order parameter and correlation times are said to accurately represent the motions of the system. The accuracy of the calculated parameters increases with shorter τ_e times and with increasing values of S^2 (Lipari & Szabo, 1982a; Dellwo & Wand, 1991). Specific guidelines for evaluating the validity of the fitted parameters determined by the model-free spectral densities are given in Lipari and Szabo (1982a,b).

$$\text{error} = \sum_{\omega1,\omega2}\left(\frac{\text{NOE}_{calc} - \text{NOE}_{exp}}{\text{NOE}_{exp}}\right)^2 + \left(\frac{T_{1,calc} - T_{1,exp}}{T_{1,exp}}\right)^2 \quad (7)$$

Table I: ^{13}C Assignments (in ppm) for Alamethicin[a]

Pro-2	α	65.7	Leu-12	α	54.05
	β	29.8		β	41.60
	γ	(27.15, 26.97)		γ	25.70
	δ	50.06		δ	23.34, 21.42
Ala-4	α	54.04	Pro-14	α	64.75
	β	17.10		β	30.10
				γ	(27.17, 26.97)
Ala-6	α	53.87		δ	50.61
	β	17.10			
			Val-15	α	64.20
Gln-7	α	58.08		β	30.47
	β	27.25		γ	20.28, 19.50
	γ	31.95			
			Gln-18	α	56.95
Val-9	α	65.80		β	32.65
	β	30.55		γ	28.10
	γ	20.91, 19.70			
			Gln-19	α	55.68
Gly-11	α	45.00		β	38.08
				γ	27.98
			Phol-20	α	54.46
				β	38.08
				β'	64.82
Aib *pro-R*	β	26.7–28.0			
Aib *pro-S*	β	23.4–24.4			

[a] All chemical shifts are relative to $^{12}CD_3OD$ at 49.0 ppm, 25 °C.

Results

Resonance Assignments. Previous carbon assignments were based on a comparison between the one-dimensional spectra of synthetic fragments and natural alamethicin, and they were not assigned to specific residues but to residue type (Schmitt & Jung, 1985; Jung et al., 1975). To make more complete assignments of the ^{13}C resonances of this peptide, the ^{1}H resonance assignments were assigned first. The assignments made here agreed with the ^{1}H assignments determined previously (Esposito et al., 1987). Having established the ^{1}H assignments, single-bond and multiple-bond ^{1}H-detected 2D NMR experiments were then used to make the residue-specific

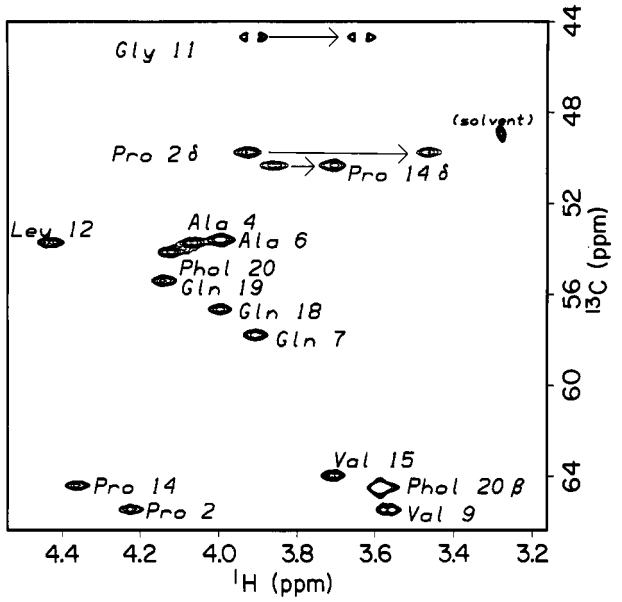

FIGURE 2: Portion of the ^1H–^{13}C correlation map depicting the α-carbon assignments for alamethicin. Heteronuclear correlations were used in the assignment of the alamethicin ^{13}C spectrum. Details of the ^1H-detected two-dimensional NMR experiment are presented under Experimental Procedures.

^{13}C resonance assignments for alamethicin in $^{12}CD_3OD$. These ^{13}C resonance assignments for natural alamethicin are shown in Table I. Shown in Figure 2 is the C^{α}–H portion of the 2D $^1H\{^{13}C\}$ correlation map with the appropriate assignments. Most of the assignments could be made from the single-bond experiment; however, ambiguous assignments brought about by unresolved ^1H resonances were determined using the multiple-bond correlation experiment. For example, the α-^1H resonances for Gln-18 and Ala-6 are at 3.99 ppm (see Figure 2); as a result, the identification of the appropriate ^{13}C resonance cannot be made using the single-bond experiment. However, the β-^1H resonances for the two residues are well resolved, and they were used in the multiple-bond experiment to confirm the appropriate α-carbon assignment.

As seen in Table I, the two Pro γ-carbons are close in chemical shift and are particularly difficult to resolve. In fact, the β-, γ-, and δ-^1H resonances between the two prolines are nearly equivalent. This similarity in resonance frequencies argues for a similarity in the local environment or conformation of the two Pro residues. Esposito et al. (1987) concluded that the Pro-2 and Pro-14 environments were similar, on the basis of the characteristic α-helical NOEs and dihedral angles measured for each residue and the similarity of the unusual temperature factors of the adjacent residues.

The resonances of the Aib β-methyl carbons show magnetic nonequivalence as indicated in Table I. This magnetic nonequivalence is indicative of their presence in an α-helix (Schmitt & Jung, 1985; Jung et al., 1983). Jung et al. (1983) demonstrated that the geminal methyl groups of Aib carbons exhibit a nonequivalence that is dependent on the type and extent of secondary structure present in peptide oligomers. Consistent with their earlier studies, the low-field group of carbons (26.5–27.5 ppm) was assigned to the *pro-R* configuration and the carbons at the higher field (23.2–24.3 ppm) to the *pro-S* configuration. This assignment reflects the positioning of the *pro-R* methyl carbon along the direction of the peptide carbonyl group in right-handed α-helices, thus deshielding it relative to the *pro-S* carbon (Jung et al., 1983).

^{13}C Spin–Lattice Relaxation Rates and NOEs. Shown in Figure 3 is a representative set of relaxation data obtained from

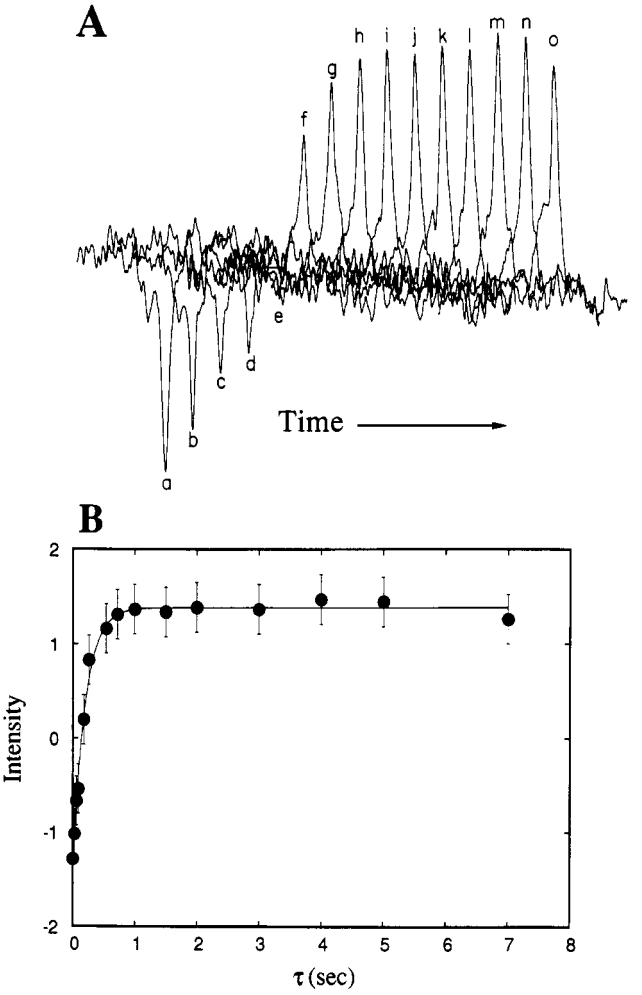

FIGURE 3: Time dependence of the magnetization for the inversion recovery sequence 180–τ–90 as a function of τ. In (A), a recording of the resonance for the Gln-19 α-carbon at 55.7 ppm is shown as a function of τ. The recordings "a–o" correspond to values of τ of 1 μs, 30, 60, 90, 180, 360, 540, and 720 ms, and 1.0, 1.5, 2.0, 3.0, 4.0, 5.0, and 7.0 s, respectively. Shown in (B) is a fit of the time dependence of the Gln-19 α-carbon resonance intensity to a single exponential.

the inversion recovery experiment described above. The spectra in Figure 3A show the recovery of the ^{13}C magnetization for the Gln-19 α-carbon of alamethicin in $^{12}CD_3OD$. Shown in Figure 3B is the fit of these data to an exponential decay. These relaxation curves were well fit by single exponentials. The T_1 experiment was carried out 3 times at each frequency, for a total of six experiments. The average values for the T_1 relaxation rates at 125 and 75 MHz are shown in Table II. Typically, the standard deviations for these values varied from less than 1% to about 4%. Also shown in Table II are the ^1H–^{13}C NOEs for alamethicin at 125 and 75 MHz. These numbers are the average of two to four experiments at each frequency, and the standard deviations were all less than 5%.

Rotational Motion of Alamethicin. The motion of alamethicin was analyzed from the relaxation rates of the α-carbons (shown in Table II) to provide an indication of the overall reorientation of the molecule in solution. The relaxation rates for five of the α-carbons could not be reliably obtained due to resonance overlap; as a result, the remaining seven protiated α-carbons were used for this analysis. This analysis utilized models for both isotropic and anisotropic overall motion with and without associated internal motions, and included the "model-free" spectral density functions described

Table II: Experimental ^{13}C T_1 and NOE Data[a]

carbon		NOE 125 MHz	NOE 75 MHz	T_1 (ms) 125 MHz	T_1 (ms) 75 MHz
Pro-2	β	1.80	1.83	504	328
	γ	2.12	2.23	581	398
	δ	1.51	2.17	442	312
Ala-4/6	α	1.62	1.96	302	170
	β	2.40	2.21	1230	971
Gln-7	β	2.03	2.13	476	256
Val-9	β	1.60	1.85	380	241
	γ	1.73	2.59	1840	1320
	γ	2.17	2.56	1380	1070
Gly-11	α	1.64	1.67	280	161
Leu-12	β	1.70	1.98	362	277
	γ	1.72	2.03	371	250
	δ	2.30	2.60	1440	1190
	δ	2.27	2.38	1970	1590
Pro-14	α	1.63	1.90	247	160
	β	1.67	2.22	497	347
	γ	1.92	2.15	666	449
	δ	1.58	1.91	400	268
Val-15	α	1.42	1.71	239	159
	β	1.68	1.80	338	256
	γ	2.14	2.23	1660	1320
	γ	2.32	2.77	1410	1080
Gln-18	α	1.64	1.76	239	159
	β	1.77	1.96	322	276
Gln-19	α	1.56	1.80	212	165
	β	1.80	1.97	341	262
Phol-20	α	1.65	1.69	318	206
	β	2.04	2.32	481	310
	β′	1.95	2.15	410	312
Aib					
pro-R	β	2.37	2.47	776	632
	β	2.37	2.64	903	626
	β	2.24	2.55	828	570
	β	2.19	2.51	812	690
pro-S	β	2.09	2.52	2490	1820
	β	1.91	2.34	2340	1600
	β	2.97	2.38	1470	1190
	β	2.35	2.58	1650	1240
	β	2.28	2.23	1560	1210

[a] The T_1 data are the average of three measurements at each frequency, and the NOE is an average of between two and four measurements at each frequency. The T_1 data have a standard deviation that ranges from less than 1% to 4%, and the NOE data have a standard deviation that ranges from 2 to 5%.

Table III: Fast Correlation Times (τ_e) and Order Parameters for Alamethicin[a]

carbon		τ_e (ps)	S^2	error
Pro-2	β	44.0	0.42	0.041
	γ	52.9	0.29	0.0090
	δ	11.2	0.55	0.043
Ala-4	β	25.7	0.10	0.0022
Ala-6	α	1.08	0.95	0.025
Gln-7	β	69.1	0.48	0.050
Val-9	β	4.99	0.70	0.0044
	γ	7.36	0.11	0.075
	γ	22.7	0.093	0.020
Gly-11	α	1.18	1.00	0.012
Leu-12	β	53.2	0.68	0.010
	γ	50.2	0.62	0.0090
	δ	24.5	0.071	0.012
	δ	16.1	0.062	0.0032
Pro-14	α	1.16	1.07	0.0076
	β	27.2	0.45	0.032
	γ	31.5	0.30	0.010
	δ	8.94	0.63	0.0077
Val-15	α	1.23	1.09	0.015
	β	35.7	0.68	0.0067
	γ	15.1	0.088	0.0025
	γ	27.4	0.071	0.028
Gln-18	α	1.24	1.09	0.00087
	β	74.8	0.59	0.022
Gln-19	α	1.29	1.15	0.014
	β	70.1	0.60	0.0062
Phol-20	α	1.03	0.82	0.0024
	β	69.6	0.36	0.025
	β′	70.6	0.43	0.0046
Aib *pro-R*	β	48.6	0.140	0.0031
		44.7	0.130	0.029
		43.8	0.160	0.027
		41.1	0.140	0.014
Aib *pro-S*	β	11.1	0.059	0.025
		7.94	0.080	0.025
		28.9	0.051	0.024
		21.8	0.067	0.014
		18.3	0.088	0.00057

[a] τ_e and S^2 were determined by fitting the relaxation and NOE data to the anisotropic spectral density (eq 5b) as described in the text. Values of $\tau_1 = 1.20$ ns, $\tau_2 = 0.20$ ns, and $A = 0.66$ were used, and the error is the value of the error function with the fitted internal motion parameters (eq 7).

under Experimental Procedures. Using the complete isotropic expression (eq 3a), the alamethicin α-carbon data could be accurately reproduced with $\tau_M = 0.610$ ns. The order parameters ranged from 0.784 for the C-terminal Phol to ≈1.0, and five of the seven α-carbon positions had values >0.95. The correlation times for the internal motions (τ_e) were in the picosecond range. The fast motions for the α-carbons satisfy the conditions $\tau_e/\tau_M < 0.01$ and $\omega\tau_e < 0.1$, indicating that the "model-free" analysis is valid (Lipari & Szabo, 1982b). Furthermore, the high value of S^2 indicates that the internal motions contribute little to the overall spectral density. This suggests that the backbone of alamethicin is very rigid. Indeed, when the internal motions are eliminated by assuming that $t_e \approx 0$ (eq 6a), τ_M is found to be 0.76 ns, a value which is close to that determined using the full spectral density function.

The data were next analyzed using a spectral density function for anisotropic overall motion, which assumed that internal motions were fast relative to the overall motion and that they were in the extreme narrowing regime (eq 5b). Using a grid search technique, a shallow but unique minimum was found at $\tau_1 = 1.2$ ns, $\tau_2 = 0.20$ ns, and $A = 0.66$. The value of the total error at this minimum was less than the minimum value found using the isotropic model (0.078 versus 0.225). The values for S^2 and τ_e that are obtained were close to the values that were found using the isotropic model (generally within 10%). Again, five of the seven order parameters for the α-carbons were very close to 1.0 with their fast correlation times ranging from 1 to 2 ps. If τ_M is equated with τ_2 and the above rules for checking the accuracy of the fitted parameters are applied, the "model-free" analysis is valid (as was the case for the isotropic model). Furthermore, the picosecond τ_e values indicate that the simplification of the spectral density function used to derive eq 4b is justified. An analysis of the data using the full anisotropic spectral density function (eq 3b) with the above τ_1, τ_2, and A values yielded nearly identical results for the values of S^2 and τ_e.

The data for the α-carbons could be accurately represented, with similar values for the minimal total error, by either the isotropic or the anisotropic spectral density. In fact, the "weighted" average of the anisotropic correlation times is nearly equal to the correlation time for isotropic motion. By application of the criteria for the "model-free" analysis, either model for overall motion appears to be appropriate. However, it is likely that alamethicin motion is most accurately represented by the anisotropic model. This model produced a unique minimum with a lower total error than was found for the isotropic model. In addition, since there is little motion along the peptide backbone, alamethicin rotational motion must be more accurately represented by the anisotropic model. For these reasons, the values for S^2 and τ_e that are presented

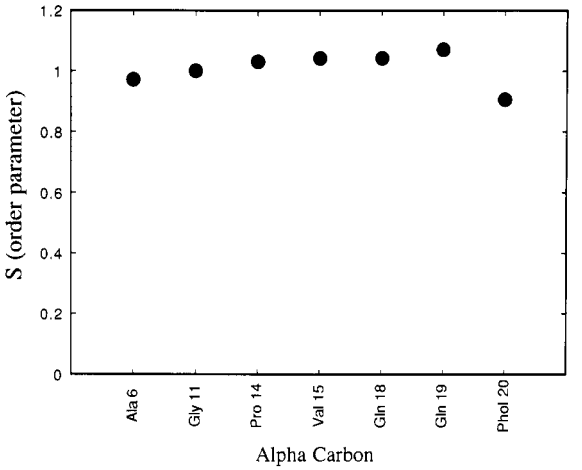

FIGURE 4: Variation of the order parameter S for the α-carbons analyzed using a model for anisotropic overall reorientation (eq 5b) with $\tau_1 = 1.2$ ns, $\tau_2 = 0.2$ ns, and $A = 0.66$. There is little variation in the values of S for the α-carbons along the length of the peptide, indicating that it behaves as a rigid rod. The rates of fast motion for each α-carbon position are nearly identical and small, also consistent with the idea that alamethicin behaves as a rod.

in Table III are those obtained from the anisotropic analysis. Shown graphically in Figure 4 is the variation of the S values with residue position for the α-carbons. The order parameter S is close to 1 along the entire length of the peptide and drops only slightly at the C- and N-termini.

It is important to note that there is likely considerable uncertainty in the values of τ_e that are listed in Table III. As indicated above, when values of S^2 are close to 1, the rates of internal motion make only a minor contribution to the relaxation rate, and are therefore poorly determined. However, the overall tumbling rates as well as the order parameters are still well-defined [see, for example, Palmer et al. (1991) and Lipari and Szabo (1982a,b)].

Internal Motions of Alamethicin Side Chains. An examination of the intraresidue order parameters in Table III shows that they follow the expected pattern of increased motional amplitude with increased distance from the backbone. Slight increases in the correlation times are observed for side chain carbons near the C-terminus; however, as discussed above, the associated α-carbons appear to be nearly rigid. These results are consistent with a rigid, helical backbone with some motional flexibility in the γ- and δ-carbons of the (linear) side chains. As with the α-carbons, there were no apparent variations in the internal motions for the side chain carbons along the peptide, and no evidence that there were regions of relative flexibility or rigidity. The order parameter data for the proline side chain carbons follow $\gamma < \beta < \delta$, a pattern which is consistent with the fact that the β- and δ-carbons are attached to backbone carbons while the γ-carbon is two bonds removed from those same carbons.

DISCUSSION

Alamethicin Is a Rigid Rod in Solution. NMR relaxation data were obtained and analyzed here in order to provide information on the molecular dynamics of alamethicin in solution. These studies were performed in methanol for several reasons; first, all previous NMR studies on alamethicin were carried out in methanol, and there is good evidence that the peptide is a monomer in methanol even at high concentrations of peptide (Esposito et al., 1987; Cascio & Wallace, 1988; Archer et al., 1991). Thus, the data presented here allow a comparison of NMR relaxation data with data obtained using other NMR experiments. More importantly, as discussed below, the solution dynamics of this peptide provide a likely indication of its dynamic behavior in the membrane. Several findings presented here provide a strong indication that alamethicin behaves as a rigid helical rod in methanol. The values of S^2 determined for the α-carbons indicate that the rapid internal motions of the peptide backbone carbons are highly restricted, regardless of the type of overall motion that is assigned to the molecule.[2] As discussed below, the overall motion of alamethicin is best fit by an anisotropic model, where the two rates for slow anisotropic tumbling in solution are close to those expected for a rigid rod that is about the size of an alamethicin monomer. In addition, an analysis of the side chain motions (discussed below) indicates that these motions are also restricted, a finding which is also consistent with the view that the backbone of alamethicin is rigid. Finally, diastereotopic differences are observed in the dynamics as well as the ^{13}C chemical shifts (for example, among the Aib β-carbons). The magnitudes of these differences provide evidence for a stable secondary structure (Jung et al., 1983; Wuthrich, 1986).

Motion in the alamethicin backbone should be easily detected by the NMR relaxation measurements made here. Recent molecular dynamics simulations of the hinge motion in triosephosphate isomerase using a rigid-body approximation for the protein and the active-site "lid" found that the hinge opening occurred within a time frame of 20–30 ps (Joseph et al., 1990). If by analogy the N- and C-termini of alamethicin are approximated as rigid bodies connected by a hinge, motions of a similar time scale should be observed for residues in this region, and would be detectable by the methods employed in this study. The picosecond effective correlation times and the high order parameters along the backbone argue against a hinge region in this molecule. Previously, a hinge region was proposed for the region near Pro-14 [see, for example, Fox and Richards (1982)]. Other evidence that argues against a hinge region at Pro-14 is the similarity in the degree of side chain motion for positions in the putative hinge region compared with positions elsewhere in the peptide. For example, Pro-14 and Pro-2 as well as Val-15 and Val-9 show similar amplitudes of side chain motion.

The view of alamethicin as a rigid and entirely helical peptide in solution is not entirely surprising. Previous evidence from X-ray and optical studies suggests that alamethicin is largely helical (Fox & Richards, 1982; Vogel, 1987). NMR data on the temperature and pH dependence of the ^1H chemical shifts, coupling constants, and NOEs also suggest that the peptide is helical and rigid (Esposito et al., 1987). Proline residues within α-helical segments are not always helix-breakers, but can frequently act as helix-benders (Sankararamakrishnan & Vishveshwara, 1990), and the data presented here demonstrate that the presence of proline residues in the alamethicin helix does not discount the possibility of an entirely helical peptide. Aib residues which are abundant in alamethicin are known to be strongly helix-stabilizing, and would also be expected to contribute to the rigidity of the alamethicin backbone (Karle & Balaram, 1990).

[2] Slow motions which do not contribute to the T_1 or NOE processes could be modulating the conformation of alamethicin. To test for this possibility, ^{13}C spin–spin relaxation rates (T_2) were measured (data not presented). These rates should be sensitive to slower motions which do not contribute to the T_1 or the NOE (Palmer et al., 1991). With the exception of the C-terminal Phol, the experimental T_2 rates for the α-carbons are very close to values that are predicted using the model for motion presented here. That is, the T_2 rates do not indicate the presence of slow motions that would contribute to T_2 but not T_1.

Relevance of Peptide Dynamics in Methanol to Peptide Dynamics in Membranes. The data obtained here for alamethicin were obtained for the peptide dispersed in solution rather than in a lipid bilayer. Nonetheless, the dynamics of alamethicin in methanol are likely to provide some insight into the dynamics of the peptide in the lipid bilayer. The results of previous studies indicate that the overall structure of the peptide is similar in methanol and in lipid bilayers. Small differences have been observed for alamethicin in these two environments and suggest that alamethicin is slightly more helical in lipid bilayers than in methanol (Harris & Chapman, 1988; Vogel, 1987). Thus, the fact that alamethicin is highly structured with a rigid backbone in methanol suggests that it is likely to be highly structured and rigid in lipid bilayers. The models for alamethicin gating that are consistent with this result are those that involve changes in the orientation of the entire alamethicin helix. Of the models that have been proposed, neither the helix bundle model of Boheim et al. (1983) nor the helix insertion model shown in Figure 1A requires flexibility in the alamethicin helix backbone. These are by no means the only models by which gating can be envisioned to occur without flexibility in the helix.

Slow Motional Rates Are Consistent with Those Expected for a Rigid Monomeric Peptide. The NMR relaxation data obtained here appeared to fit well to values for slow and fast correlation times and order parameters using the model-free approach. A number of features of the results and the data presented in Table III are physically reasonable and lend credibility to the procedure used to analyze the relaxation data. Using the anisotropic model for the overall motion of alamethicin, two correlation times describing the motion were obtained, $\tau_1 = 1.2$ ns and $\tau_2 = 0.20$ ns. These values are close to the τ_M value of 0.72 ns estimated by using ^{1}H NOE data for the Pro-2 δ-protons (Esposito et al., 1987). In addition, these correlation times appear to be physically reasonable. If alamethicin rotates anisotropically, the rotational diffusion constants can be estimated using Perrin's equations by assuming that its shape approximates a prolate ellipsoid (Cantor & Schimel, 1980). Using as dimensions the values determined by dielectric relaxation measurements, 35 Å × 13 Å (Schwarz & Savko, 1982), values of $\tau_1 = 1.18$ ns and $\tau_2 = 0.649$ ns are obtained.[3] These are very close in magnitude to the correlation times obtained using the ^{13}C NMR data, even though the experimental correlation times suggest a much large axial ratio (closer to 6) than are obtained in the dielectric relaxation measurements. These data also provide strong evidence that alamethicin does not aggregate in methanol even at the high concentrations of peptide examined here.

Internal Motions Are Also Consistent with a Rigid Backbone. As described above, the side chain carbons had internal motions that increased in amplitude and decreased in rate as the distance from the peptide backbone increased, a result that is physically reasonable. The order parameters for the side chain should reflect the amplitudes of fast motions in the side chains such as bond isomerizations and torsions. Using a simple model that describes the motion of the side chains where the dynamics are modeled as a series of independent rotations, the values of S^2 should be the following: C_β, 0.111; C_γ, 0.0123; C_δ, 0.00136 (Wallach, 1967). When these expected values are compared with the values of S^2 shown in Table III (for example, see Val-9, Leu-12, or Val-15), it is clear that the experimental results, while following the pattern of decreasing S^2, decrease much less than expected as a function of distance from the backbone. This indicates that the motion of these side chains is restricted and does not undergo uncorrelated motion.

[3] The values for τ_1 and τ_2 were calculated using Perrin's equations as given in Cantor and Schimmel (1980). First, $f_{rot} = 6\eta V_h$ was evaluated where $V_h = 1.338 \times 10^{-21}$ cm^3 on the basis of $d_1 = 0.3$ g of H_2O/g of protein and $V_2 = 0.7$ cm^3 g^{-1}, then, τ_r was calculated as $\tau_r = f_{rot}/2kT$. Structure factors of $F_a = 0.783$ and $F_b = 2.061$ were calculated for a prolate ellipsoid with $p = b/a = 0.371$ (Schwarz & Savko, 1982). The correlation times for motion about each axis were then evaluated as $\tau_1 = \tau_r F_b$ and $\tau_b = \tau_r(2/f_{rot})[(F_a f_{rot})^{-1} + (F_b f_{rot})^{-1}]^{-1}$.

Table IV: Methyl Group Dynamics of Alamethicin

carbon	S^2	S^2_{axis}	θ_0[a]	γ_0[b]
Val-9 γ-1	0.110	0.991		6.0
Val-9 γ-2	0.093	0.838		26.0
Val-15 γ-1	0.088	0.793		30.5
Val-15 γ-2	0.071	0.640		41.0
Ala-4 β	0.102	0.919	19.1	
Leu-12 δ-1	0.071	0.640		41.0
Leu-12 δ-2	0.062	0.559		48.5
pro-S Aib β	0.059	0.532	49.7	
	0.080	0.721	36.8	
	0.051	0.459	54.5	
	0.067	0.604	45.0	
	0.088	0.793	31.2	

[a] The value of θ_0 is that obtained from the diffusion of the methyl symmetry axis in a cone and is calculated from the value of S^2_{axis} using the expression $S^2_{axis} = S^2_{cone} = (1/2)(1 + \cos\theta_0)\cos\theta_0$. [b] The restriction angle, γ_0, is calculated from S^2_{axis} using the expression $S^2_{axis} = S^2_{restr} = P_2(\cos\beta')^2 + 3\sin^2\beta'\sin^2\gamma_0[\cos^2\beta' + (1/4)\sin^2\beta'\cos^2\gamma_0]\gamma_0^2$ where β' has a value of 70.5°.

Some insight into the nature of more complex side chain motions can be obtained from an analysis of methyl group rotation. As described previously (Woessner, 1962), when $S^2 < 0.111$ the motion of the methyl symmetry axis can be characterized by $S^2 = 0.111S^2_{axis}$, where S^2_{axis} is the order parameter of the methyl symmetry axis. The values of S^2_{axis} that are obtained from the experimental values of S^2 can be interpreted in terms of different models for the motion of the methyl symmetry axis. One model that is appropriate for Ala and Aib β-carbons involves the diffusion of a director in a cone of semiangle θ_0, where the director is the methyl symmetry axis (Lipari & Szabo, 1980). In this model, the director is allowed to diffuse within a cone of semiangle θ_0, which can be calculated from the value of S^2_{axis} (see legend of Table IV). Another model that can be used is that of restricted diffusion, and it may be more appropriate for the more extended side chains of Val and Leu (London & Avitable, 1978; Wittebort & Szabo, 1978). Here, the methyl group is allowed to rotate freely about its symmetry axis, but motion about the preceding C–C bond is restricted. In this case, the value of S^2_{axis} is used to calculate the restriction angle, γ_0. Values for θ_0 and γ_0 are summarized in Table IV. The degree of restriction for the methyl carbons, as described by the angles θ_0 or γ_0, follows the expected pattern with chain position, that is, Ala < Val < Leu. Stereospecific differences in restriction are observed for Val-9 and -15 γ-carbons as well as the two Aib β-carbons. In general, all motions are fairly restricted, indicating a high degree of rigidity in the secondary structure.

The *pro-R* Aib methyl groups have order parameters greater than 0.111; therefore, they could not be analyzed in terms of a diffusion or restriction angle. Jung et al. (1983) previously noted the difference in T_1 relaxation between the *pro-R* and *pro-S* methyls in alamethicin as well as a number of related Aib-containing peptides. The *pro-S* methyl groups occupy positions similar to those of a typical Ala methyl group in an α-helix. The *pro-R* methyl groups occupy positions analogous to the C$^\alpha$-proton of the common amino acids and therefore point inward toward the helix axis. This is consistent with the restriction of *pro-R* methyl motion about the symmetry axes

indicated by the *pro-R* order parameters ($S^2 > 0.111$) shown in Table III. This finding is also consistent with the existence of a rigid helical structure over the entire length of the peptide.

In conclusion, the dynamics of the peptide ion channel alamethicin were evaluated by studying the ^{13}C T_1 relaxation rates and ^{13}C–^1H NOEs for the peptide in methanol at two magnetic field strengths. The model-free approach of Lipari and Szabo was employed to fit the data with values for the overall rotational correlation times and to characterize the rate (τ_e) and amplitude (S) of the internal peptide motions. The results presented here indicate that the overall rotation can be fit well by an anisotropic spectral density function. The results provide direct evidence from the amplitudes of internal motions and indirect evidence from the side chain dynamics that alamethicin behaves as a "rigid" rod in solution. That is, the backbone appears to lack any significant segmental motion or bending along the peptide backbone in the picosecond time scale. This finding for the peptide in solution suggests that it is unlikely to have a flexible backbone in the membrane and the most likely models for the gating will be those in which the entire alamethicin helix reorients in the membrane electric field.

References

Archer, S. J., & Cafiso, D. S. (1991) *Biophys. J. 60*, 380.

Archer, S. J., Ellena, J. F., & Cafiso, D. S. (1991) *Biophys. J. 60*, 389.

Banerjee, U., & Chan, S. I. (1983) *Biochemistry 22*, 3709.

Banerjee, U., Tsui, F. P., & Balasubramanian, T. N. (1983) *J. Mol. Biol. 165*, 757.

Bauman, G., & Mueller, P. (1974) *J. Supramol. Struct. 2*, 538.

Bax, A., & Davis, D. G. (1985) *J. Magn. Reson. 65*, 335.

Bax, A., & Summers, M. F. (1986) *J. Am. Chem. Soc. 106*, 2093.

Bax, A., Ikura, M., Kay, L. E., & Zhu, G. (1991) *J. Magn. Reson. 91*, 174.

Boheim, G. (1974) *J. Membr. Biol. 19*, 277.

Boheim, G., Hanke, W., & Jung, G. (1983) *Biophys. Struct. Mech. 9*, 181.

Braunschweiler, L., & Ernst, R. R. (1983) *J. Magn. Reson. 53*, 521.

Brooks, C. L., Karplus, M., & Pettitt, B. M. (1988) *Adv. Chem. Phys. 71*, 1.

Brunger, A. T., Huber, R., & Karplus, M. (1987) *Biochemistry 26*, 5153.

Cantor, C. R., & Schimmel, P. R. (1980) in *Biophysical Chemistry. Part II: Techniques for the Study of Biological Structure and Function*, pp 500, 560, W. H. Freeman, San Francisco.

Cascio, M., & Wallace, B. A. (1988) *Proteins: Struct., Funct., Genet. 4*, 89.

Clore, G. M., Driscoll, P. C., Wingfield, P. T., & Gronenborn, A. M. (1990) *Biochemistry 29*, 7387.

Dellwo, M. J., & Wand, A. J. (1989) *J. Am. Chem. Soc. 111*, 4571.

Dellwo, M. J., & Wand, A. J. (1991) *J. Magn. Reson. 91*, 505.

Esposito, G., Carver, J. A., Boyd, J., & Campbell, I. D. (1987) *Biochemistry 26*, 1043.

Fox, R. O., & Richards, F. M. (1982) *Nature 25*, 325.

Fringeli, U. P., & Fringeli, M. (1979) *Proc. Natl. Acad. Sci. U.S.A. 76*, 3852.

Haberkorn, R., Ruben, D., & States, D. J. (1982) *J. Magn. Reson. 48*, 286.

Hall, J. E., Vodyanoy, I., Balasubramanian, T. M., & Marshall, G. R. (1984) *Biophys. J. 45*, 233.

Harris, P. I., & Chapman, D. (1988) *Biochim. Biophys. Acta 943*, 375.

Henry, G. D., Weiner, J. H., & Sykes, B. D. (1986) *Biochemistry 25*, 590.

Joseph, D., Petsko, G. A., & Karplus, M. (1990) *Science 249*, 1425.

Jung, G., Dubischar, N., & Leibfritz, D. (1975) *Eur. J. Biochem. 54*, 395.

Jung G., Bruckner, H., Bosch, R., Winter, W., Schall, H., & Strahle, J. (1983) *Liebigs Ann. Chem.*, 1096.

Karle, I. L., & Balaram, P. (1990) *Biochemistry 29*, 6746.

Karplus, M., & Dobson, C. M. (1986) *Methods Enzymol. 131*, 362.

Kay, L. E., Torchia, D. A., & Bax, A. (1989) *Biochemistry 28*, 8972.

Lindman, B., Soderman, O., & Wennerstrom, H. (1987) *Surfactant Sci. Ser. 22*, 295.

Lipari, G., & Szabo, A. (1980) *Biophys. J. 30*, 489.

Lipari, G., & Szabo, A. (1981a) *Biochemistry 20*, 6250.

Lipari, G., & Szabo, A. (1981b) *J. Chem. Phys. 75*, 2971.

Lipari, G., & Szabo, A. (1982a) *J. Am. Chem. Soc. 104*, 4546.

Lipari, G., & Szabo, A. (1982b) *J. Am. Chem. Soc. 104*, 4559.

London, R. E., & Avitable, J. (1978) *J. Am. Chem. Soc. 100*, 7159.

Mayer, C., Grobner, G., Muller, K., Weisz, K., & Kothe, G. (1990) *Chem. Phys. Lett. 165*, 155.

Menestrina, G., Voges, K.-P., Jung, G., & Boheim, G. (1986) *J. Membr. Biol. 93*, 111.

Palmer, A. G., Rance, M., & Wright, P. E. (1991) *J. Am. Chem. Soc. 113*, 4371.

Piantini, U., Sorensen, O. W., & Ernst, R. R. (1982) *J. Am. Chem. Soc. 104*, 6800.

Rance, M. (1987) *J. Magn. Reson. 74*, 557.

Sankararamakrishnan, R., & Vishveshwara, S. (1990) *Biopolymers 30*, 281.

Schmitt, H., & Jung, G. (1985) *Liebigs Ann. Chem.*, 345.

Schwarz, G., & Savko, P. (1982) *Biophys. J. 39*, 211.

Schwarz, G., Stankowski, S., & Rizzo, V. (1986) *Biochim. Biophys. Acta 861*, 141.

Shaka, A. J., Barker, P. B., & Freeman, R. (1985) *J. Magn. Reson. 64*, 547.

Vogel, H. (1987) *Biochemistry 26*, 4562.

Wallach, D. (1967) *J. Chem. Phys. 47*, 5258.

Weaver, A. J., Kemple, M. D., & Prendergast, F. G. (1988) *Biophys. J. 54*, 1.

Weaver, A. J., Kemple, M. D., & Prendergast, F. G. (1989) *Biochemistry 28*, 8624.

Wille, B., Franz, B., & Jung, G. (1989) *Biochim. Biophys. Acta 986*, 47.

Williams, R. J. P. (1989) *Eur. J. Biochem. 183*, 479.

Wittebort, R. J., & Szabo, A. (1978) *J. Chem. Phys. 69*, 1722.

Woessner, D. E. (1962) *J. Chem. Phys. 36*, 1.

Wuthrich, K. (1986) in *NMR of Proteins and Nucleic Acids*, John Wiley & Sons, New York.